

Near-Optimal Sensor Placement for Inverse Problems

Juri Ranieri*, *Student Member, IEEE*, Amina Chebira†, *Member, IEEE* and Martin Vetterli*, *Fellow, IEEE*

Abstract—A classic problem is the estimation of a set of parameters from measurements collected by a set of sensors. The number of sensors is often limited by physical or economical constraints and their placement is of fundamental importance to obtain accurate estimates.

Unfortunately, the selection of the optimal sensor locations is intrinsically combinatorial and the available approximation algorithms are not guaranteed to generate good solutions in all cases of interest.

We propose SmartSense, a greedy algorithm for the selection of optimal sensor locations. The cost function at the heart of the algorithm is the *frame potential*, a scalar property of matrices that measures the orthogonality of its rows. Notably, SmartSense is the first algorithm in the literature that is near-optimal w.r.t. the mean square error, meaning that the solution is always guaranteed to be close to the optimal one.

Moreover, we show with an extensive set of numerical experiments that SmartSense achieves the state-of-the-art performance while having the lowest computational cost, when compared to other greedy methods.

Index Terms—sensor placement, inverse problem, frame potential, greedy algorithm,

I. INTRODUCTION

In many contexts, it is of interest to measure physical phenomena that vary in space and time. Common examples are temperature, sound, and pollution. Modern approaches tackling this problem are often based on wireless sensor networks (WSN), that are systems composed of many sensing nodes, each capable of measuring, processing and communicating information about the surrounding environment.

Challenges and trade-offs characterize the design of a WSN. One of the key aspects to design a successful WSN is the optimization of the spatial locations of the sensors nodes, given its impact on many relevant indicators, such as coverage, energy consumption and connectivity. When the data collected by the WSN is used to solve inverse problems, the optimization of the sensor locations is even more critical. In fact, the location of the sensor nodes determines the error in the solution of the inverse problem and its optimization represents the difference between being able to obtain a reasonable solution or not. In this work, we consider linear inverse problems defined as

$$\mathbf{f} = \Psi\alpha, \quad (1)$$

where $\mathbf{f} \in \mathbb{R}^N$ is the measured physical field¹, $\alpha \in \mathbb{R}^K$ are the parameters to be estimated and $\Psi \in \mathbb{R}^{N \times K}$ is the

* School of Computer and Communication Sciences, Ecole Polytechnique Fédérale de Lausanne (EPFL), CH-1015 Lausanne, Switzerland (contact e-mail juri.ranieri@epfl.ch).

† Swiss Center for Electronics and Microtechnology (CSEM), CH-2000 Neuchâtel, Switzerland.

¹The physical field is generally continuous in time and space, but we consider its discrete version throughout the paper.

known linear model representing the relationship between the measurements and the parameters. Note that this simple model can be easily adapted to more complicated scenarios. For example, if the collected measurements are linear combinations of the physical field, as in the presence of a sampling kernel, we can just consider $\Psi = \Phi\Theta$, where Φ and Θ represents the sampling kernel and the physical phenomenon, respectively.

The role of α depends on the specific inverse problem. For example, if the WSN is designed for *source localization*, α represents the location and the intensity of the field sources. On the other hand, if we are planning to *interpolate* the measured samples to recover the entire field, we may think of α as its low-dimensional representation. In other scientific applications, for example [1–3], the solution of a linear inverse problem is just a step inside a complex procedure and α may not have a direct interpretation. Nonetheless, the accurate estimation of α is of fundamental importance.

It is generally too expensive or even impossible to sense the physical field \mathbf{f} with N sensor nodes, where N is determined by the resolution of the discrete physical field. Assume we have only $L < N$ sensors, then we need to analyze how to choose the L sampling locations such that the solution of the linear inverse problem (1) has the least amount of error. Namely, we would like to choose the *most informative* L rows of Ψ out of the N available ones. One could just adopt a brute force approach and inspect all the possible combinations for the L sensor locations. The operation count, due to its combinatorial nature, will be exponential making the approach unfeasible even for moderate N .

It is possible to significantly reduce the computational cost by accepting a sub-optimal sensor allocation produced by an approximation algorithm. In this case, near-optimal algorithms are desired, meaning that they produce *always* a solution of *guaranteed quality*². We measure this quality as the ratio between the value of the approximated solution and the value of the optimal one, and we call it *approximation factor*.

A. Problem Statement and Prior Art

We consider the linear model introduced in (1) and a WSN measuring the field at only $L < N$ locations. We denote the set of measured locations and of available locations as $\mathcal{L} = \{i_1, \dots, i_L\}$ and $\mathcal{N} = \{1, \dots, N\}$, respectively. Note that $\mathcal{L} \subseteq \mathcal{N}$ and $|\mathcal{L}| = L$.

The measured field is denoted as $\mathbf{f}_{\mathcal{L}} \in \mathbb{R}^L$, where the subscript represents the selection of the elements of \mathbf{f} indexed by \mathcal{L} . Consequently, we define a pruned matrix $\Psi_{\mathcal{L}} \in \mathbb{R}^{L \times K}$,

²While the interest is often on the average error, here we want to make sure that all the outcomes are of a good quality.

where we kept only the rows of Ψ indexed by \mathcal{L} . We obtain a smaller linear system of equations,

$$\mathbf{f}_{\mathcal{L}} = \Psi_{\mathcal{L}} \boldsymbol{\alpha}, \quad (2)$$

where we still recover $\boldsymbol{\alpha}$, but with a reduced set of measurements, $L \geq K$. Note that, by definition we have $\Psi_{\mathcal{N}} = \Psi$ and $\mathbf{f}_{\mathcal{N}} = \mathbf{f}$.

Given the set of measurements $\mathbf{f}_{\mathcal{L}}$, there may not exist an $\hat{\boldsymbol{\alpha}}$ that solves (2). If it exists, the solution may not be unique. To overcome this problem, we usually look for the least square solution, defined as $\hat{\boldsymbol{\alpha}} = \arg \min_{\boldsymbol{\alpha}} \|\Psi_{\mathcal{L}} \boldsymbol{\alpha} - \mathbf{f}_{\mathcal{L}}\|_2^2$. This solution is found using the Moore-Penrose pseudoinverse,

$$\hat{\boldsymbol{\alpha}} = \Psi_{\mathcal{L}}^+ \mathbf{f}_{\mathcal{L}},$$

where $\Psi_{\mathcal{L}}^+ = (\Psi_{\mathcal{L}}^* \Psi_{\mathcal{L}})^{-1} \Psi_{\mathcal{L}}^*$. The pseudoinverse generalizes the concept of inverse matrix to non-square matrices and is also known as the *canonical dual frame* in frame theory. For simplicity of notation, we introduce $\mathbf{T}_{\mathcal{L}} = \Psi_{\mathcal{L}}^* \Psi_{\mathcal{L}} \in \mathbb{R}^{K \times K}$, a hermitian-symmetric matrix that strongly influences the reconstruction performance. More precisely, the error of the least square solution depends on the spectrum of $\mathbf{T}_{\mathcal{L}}$. More precisely, when the measurements $\mathbf{f}_{\mathcal{L}}$ are perturbed by a zero-mean i.i.d. Gaussian noise with variance σ^2 , the mean square error (MSE) of the least square solution [4] is

$$\text{MSE}(\hat{\boldsymbol{\alpha}}) = \|\hat{\boldsymbol{\alpha}} - \boldsymbol{\alpha}\|_2 = \sigma^2 \sum_{k=1}^K \frac{1}{\lambda_k}, \quad (3)$$

where λ_k is the k th eigenvalue of the matrix $\mathbf{T}_{\mathcal{L}}$. We thus state the sensor allocation problem as follows.

Problem 1. Given a matrix $\Psi \in \mathbb{R}^{N \times K}$ and a number of sensors L , find the sensor placement \mathcal{L} such that

$$\begin{aligned} \arg \min_{\mathcal{L}} \quad & \sum_{k=1}^K \frac{1}{\lambda_k} \\ \text{subject to} \quad & |\mathcal{L}| = L \end{aligned}$$

Note that if $\mathbf{T}_{\mathcal{L}}$ is rank deficient, that is $\text{rank}(\mathbf{T}_{\mathcal{L}}) < K$, the MSE is not bounded.

A trivial choice would be to design algorithms minimizing directly the MSE with some approximation procedure, such as greedy ones. In practice, the MSE is not used because it has many unfavorable local minima. Therefore, the research effort is focused in finding tight proxies of the MSE that can be efficiently optimized. In what follows, we survey different approximation strategies and considered proxies from the literature.

B. Prior work

Classic solutions to the sensor allocation problem can be classified in three categories: convex optimization, greedy methods and heuristics.

Convex optimization methods [5, 6] are based on the relaxation of the boolean constraints $\{0, 1\}^N$ representing the sensor placement to the convex set $[0, 1]^N$. This relaxation is usually not tight, heuristics are needed to choose the sensor locations and there is no a-priori guarantee about the distance

from the optimal solution. The authors in [6] define an online bound for the quality of the obtained solution by looking at the gap between the primal and the dual problem.

Heuristic methods [7–12] are valid options to reduce the cost of the exhaustive search, which has prohibitive cost. Again, even if the methods work in practice, little can be said about the quality or the optimality of the solution.

Greedy algorithms leveraging the submodularity of the cost function [13] are a class of algorithms having polynomial complexity and guaranteed performance w.r.t. the chosen cost function [5, 14–16]. Since the MSE is not submodular in the general case [15], alternative cost functions have been considered. The proposed methods are theoretically near-optimal w.r.t. the chosen cost function, but little can be said about the achieved MSE. Moreover, the local optimization of the proposed cost functions are computationally demanding, often requiring the inversion of large matrices [14]. Therefore, approximations of the cost functions have been proposed [14], offering a significant speedup for an acceptable reduction of the solution's quality.

Beside the approximation strategy, the approximation algorithms are differentiated by the chosen cost function. Under restrictive assumptions, the MSE can be chosen as a cost function, see [15, 17]. Common proxies of the MSE are inspired by information theoretic measures such as entropy [12], cross-entropy [16, 18] and mutual information [14]. A popular choice is the minimization of the log volume (or mean radius) of the confidence ellipsoid given by the measurements, being also the determinant of $\mathbf{T}_{\mathcal{L}}$. This proxy has been historically introduced in D-Optimal experiment design [19], but has also been successfully proposed as a cost function for a convex relaxed method [6] and greedy algorithms [5]. Other proxies have also been introduced in optimal experiment design, such as maximization of the smallest eigenvalue λ_K (E-Optimal design) or the maximization of the trace of $\mathbf{T}_{\mathcal{L}}$ (T-Optimal design). A detailed description of the different choices available for experiment design can be found in [19].

Note that in some specific scenarios, optimal strategies with a reasonable computational cost are known in literature. This is the case when we have the freedom of designing completely the matrix $\Psi_{\mathcal{L}}$, given the dimensions L and K . More precisely, if $L = K$, the optimal matrix is an orthonormal basis, while if $L > K$, we are looking for a unit-norm³ tight frame [20, 21]. Benedetto et al. showed that each tight frame is a non-unique global minimizer of the *frame potential* (FP), that is a scalar property of the frame defined as

$$\text{FP}(\Psi_{\mathcal{L}}) = \sum_{i,j \in \mathcal{L}} |\langle \boldsymbol{\psi}_i, \boldsymbol{\psi}_j \rangle|^2,$$

where $\boldsymbol{\psi}_i$ is the i th row of Ψ . One of the reasons of the popularity of FP in the frame theory community is its interesting physical interpretation [22]. Namely, it is the potential energy of the so-called *frame force*, a force between vectors inspired by the Coulomb force. The frame force and its potential energy have been introduced for its *orthogonality encouraging*

³Unit norm condition can be relaxed, but it must be substitute by a bound on the maximum sum of the eigenvalues of $\mathbf{T}_{\mathcal{L}}$.

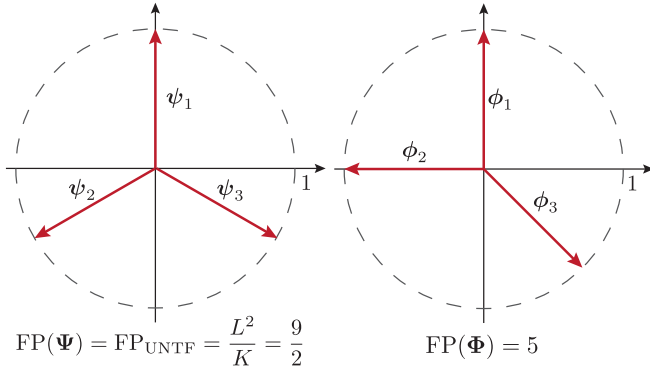


Fig. 1. A graphical representation of the unit-norm rows of two matrices Ψ and Φ . On the left, the rows Ψ are optimally spread on \mathbb{R}^2 minimizing the FP and the MSE. This is also known as the Mercedes-Benz frame and is a typical example of a unit-norm tight frame. On the right, we represent the rows of Ψ , that is a frame built by adding a vector to the orthonormal basis of \mathbb{R}^2 [ϕ_1, ϕ_2]. The three vectors are not minimizing the FP and therefore they are not in equilibrium w.r.t. the frame force. You can envision a parallel example with three electrons on a unit circle under the Coulomb force. More precisely, if the three electrons are free to move, they would reach an equilibrium when located as the vectors of Ψ , up to a rotation factor.

property: the force is repulsive when the angle between the two vectors is acute, null when they are orthogonal and attractive when the angle is obtuse. A graphical explanation of the physical interpretation is given in Figure 1, where the unit-norm rows of two matrices Ψ and Φ belonging to $\mathbb{R}^{3 \times 2}$ are represented. While Ψ , that is the unit-norm tight frame minimizing the FP, has vectors as spread as possible and therefore in equilibrium w.r.t. the frame force, the vectors Φ are not optimally spread and the FP is thus not minimized. Note that, according to frame theory, Ψ is the matrix that achieves also the minimum MSE.

Given its interpretation and its role in defining the existence of tight frames—the optimal frames in terms of MSE—we hypothesize that the FP is an interesting cost function for an approximation algorithm.

C. Our contributions

We propose SmartSense, a greedy sensor allocation method that minimizes the frame potential to choose the sensing locations \mathcal{L} . We briefly summarize the innovative aspects of the proposed algorithm,

- Under some stability conditions regarding the spectrum of Ψ , SmartSense is the only known algorithm, to the best of our knowledge, that is near-optimal w.r.t. MSE.
- SmartSense outperforms other greedy algorithms available in the literature in terms of MSE.
- SmartSense is on par with the method based on convex relaxation [6], which uses many heuristics to improve the local solution and has a significantly higher computational cost.
- The computational cost of SmartSense is significantly lower w.r.t. the other considered algorithms.

The remainder of the paper uses the following notations: calligraphic letters as \mathcal{C} indicate sets of elements, while bold letters as Ψ and ψ indicates matrices and vectors, respectively.

The i -th largest eigenvalue of $\mathbf{T}_{\mathcal{L}} = \Psi_{\mathcal{L}}^* \Psi_{\mathcal{L}}$ is denoted as λ_i . Moreover, we always consider a real physical field \mathbf{f} and real matrices Ψ for simplicity's sake, but the extension to the complex domain is easy with proper adjustments.

The content is organized as follows. In Section II we introduce some frame theory concepts focusing on the role of the FP. We describe SmartSense and the analysis of its near-optimality in Section III and we numerically compare its performance with the algorithms proposed in the scientific literature in Section IV.

II. THE FRAME POTENTIAL IN FRAME THEORY

This section briefly introduces some of the basic concepts of frame theory, that are useful to understand and analyze the proposed algorithm. Frame theory studies and designs families of matrices $\Psi_{\mathcal{L}}$ such that $\mathbf{T}_{\mathcal{L}}$ is well-conditioned. More precisely, $\Psi_{\mathcal{L}}$ is a frame for a Hilbert space \mathbb{H} if there exists two scalars A and B such that $0 < A \leq B < \infty$ satisfying for every $\mathbf{x} \in \mathbb{H}$

$$A\|\mathbf{x}\|_2^2 \leq \|\Psi_{\mathcal{L}}\mathbf{x}\|_2^2 \leq B\|\mathbf{x}\|_2^2,$$

where A and B are called frame bounds and $\Psi_{\mathcal{L}}$ is a tight frame when $A = B$. Of particular interest is the case of unit norm tight frames (UNTF); these are tight frames whose frame elements—the rows ψ —have unit norm. These provide Parseval-like relationships, despite the non-orthogonality of the frame elements of $\Psi_{\mathcal{L}}$. In addition to (3), there are other interesting relationships between the characteristics of $\Psi_{\mathcal{L}}$ and the spectrum of $\mathbf{T}_{\mathcal{L}}$. For example, we can express the FP as

$$\text{FP}(\Psi_{\mathcal{L}}) = \text{Trace}(\mathbf{T}_{\mathcal{L}}^* \mathbf{T}_{\mathcal{L}}) = \sum_{k=1}^K |\lambda_k|^2.$$

Moreover, the sum of the eigenvalues of $\mathbf{T}_{\mathcal{L}}$ is equal to the sum of the norm of the rows, $\sum_{i=1}^L \|\psi_i\|^2 = \sum_{k=1}^K \lambda_k$.

These quantities of interest take a simplified analytical form for UNTFs. In this scenario, we know [21] that the FP is minimum w.r.t. all the other matrices of the same size with unit-norm rows and it is equal to $\text{FP}_{\text{UNTF}} = \frac{L^2}{K}$. According to [21], the optimal MSE is also achieved when the FP is minimized and it is equal to $\text{MSE}_{\text{UNTF}} = \frac{K^2}{L}$. Note that in this case all the eigenvalues are equal, $\lambda_{\text{UNTF}} = \lambda_i = \frac{L}{K} \forall i$.

Next, we would like to intuitively explain why FP is a good candidate to be a proxy for the MSE. Consider the distance between the FP of a matrix with unit-norm rows $\Psi_{\mathcal{L}} \in \mathbb{R}^{L \times K}$ and the FP of a unit-norm tight frame. Then, it is possible to show that this distance is always positive and equal to

$$\text{FP}(\Psi_{\mathcal{L}}) - \text{FP}_{\text{UNTF}} = \sum_{k=1}^K \left(\lambda_k - \frac{L}{K} \right)^2,$$

where $\frac{L}{K}$ is the value of the eigenvalues λ_{UNTF} . Note that if we minimize the FP of $\Psi_{\mathcal{L}}$, then each λ_k converge to $\frac{L}{K}$.

At the same time, the distance between the MSE of $\Psi_{\mathcal{L}}$

and the MSE of the tight frame can be expressed as

$$\text{MSE}(\Psi_{\mathcal{L}}) - \text{MSE}_{\text{UNTF}} = \sum_{k=1}^K \left(\frac{1}{\lambda_k} - \frac{K}{L} \right).$$

Now, it is easy to see that if the eigenvalues converge to $\frac{L}{K}$, then $\text{MSE}(\Psi_{\mathcal{L}})$ converges to the MSE of a UNTF, being also the optimal one [21].

III. SMARTSENSE: A NEAR-OPTIMAL SENSOR PLACEMENT

Even if the intuition given in Section II is clear, it does not directly explain why an algorithm optimizing the FP allocates the sensors with some guarantees in terms of MSE. For example, we need to address some complications, such as matrices Ψ having rows with different norms and the non-uniform convergence of the eigenvalues. In what follows, we first describe the details of SmartSense and then we analyze its near-optimality in terms of both the FP and the MSE.

A. The algorithm

SmartSense finds the sensor locations \mathcal{L} given the known model Ψ and the number of available sensors nodes L with a greedy minimization of the FP. It is a greedy “worst-out” algorithm: at each iteration it removes the row of Ψ that maximally increases the FP. In other words, we define a set of locations \mathcal{S} that are not suitable for sensing and at each iteration we add to \mathcal{S} the row that maximizes the following cost function,

$$F(\mathcal{S}) = \text{FP}(\Psi) - \text{FP}(\Psi_{\mathcal{N} \setminus \mathcal{S}}). \quad (4)$$

The pseudo-code for SmartSense is given in Algorithm 1.

Algorithm 1 SmartSense

Require: Linear Model Ψ , Number of sensors L

Ensure: Sensor locations \mathcal{L}

- 1) Initialize the set of locations, $\mathcal{L} = \emptyset$.
 - 2) Initialize the set of available locations, $\mathcal{N} = \{1, \dots, N\}$.
 - 3) Find the first two rows to eliminate, $\mathcal{S} = \arg \max_{i,j \in \mathcal{N}} |\langle \psi_i, \psi_j \rangle|^2$.
 - 4) Update the available locations, $\mathcal{L} = \mathcal{N} \setminus \mathcal{S}$.
 - 5) **Repeat until L locations are found**
 - a) If $|\mathcal{S}| = N - L$, stop.
 - b) Find the optimal row, $i^* = \arg \min_{i \in \mathcal{L}} F(\mathcal{S} \cup i)$.
 - c) Update the set of removed locations, $\mathcal{S} = \mathcal{S} \cup i^*$.
 - d) Update the available locations, $\mathcal{L} = \mathcal{L} \setminus i^*$.
-

One may ask why we do not optimize directly the MSE instead of minimizing the FP which indirectly optimizes the MSE. As we have already indicated, a greedy algorithm optimizing a general function, like the MSE, converges to a local stationary point of the cost function and we have no guarantee about the distance from the global optimum. On the other hand, we can prove that SmartSense is near-optimal w.r.t. the FP exploiting the submodularity of the cost function. Then, the mathematical link between FP and MSE allows us to guarantee the performance of SmartSense also in terms of the MSE.

B. Near-optimality of SmartSense w.r.t. FP

We define the performance of SmartSense w.r.t. FP, using the theory of submodular functions. We start by defining the concept of submodularity that relates to the concept of diminishing returns: if we add an element to a set \mathcal{Y} , the benefit is smaller or equal than adding the same element to one of the subsets of \mathcal{Y} . Then, we introduce a theorem due to Nemhauser et al. [13] that defines the approximation factor of greedy algorithms maximizing a submodular function. We continue by showing that SmartSense satisfies the conditions of Nemhauser’s theorem and we derive its approximation factor in terms of FP.

Definition 1 (Submodular function). *Given two sets \mathcal{X} and \mathcal{Y} such that $\mathcal{X} \subset \mathcal{Y} \subset \mathcal{N}$ and given an element $i \in \mathcal{N} \setminus \mathcal{Y}$, a function G is submodular if it satisfies*

$$G(\mathcal{X} \cup i) - G(\mathcal{X}) \geq G(\mathcal{Y} \cup i) - G(\mathcal{Y}) \quad (5)$$

Submodular functions are useful in combinatorial optimization because greedy algorithms have favorable properties when optimizing a function with such property. More precisely, it has been proved that the greedy maximization of submodular functions is near-optimal [13].

Theorem 1 (Near-optimal maximization of submodular function [13]). *Let G be a normalized, monotone, submodular set function over a finite ground set \mathcal{N} . Let \mathcal{L} be the set of the first L elements chosen by the greedy algorithm, and let $\text{OPT} = \max_{\mathcal{A} \subset \mathcal{N}, |\mathcal{A}|=L} G(\mathcal{A})$ be the optimal set of elements. Then*

$$G(\mathcal{L}) \geq \left(1 - \frac{1}{e}\right) G(\text{OPT}),$$

where e is the Euler’s number.

Namely, if G satisfies the conditions of Theorem 1, then the solution of the greedy algorithm is always close to the optimal one. These conditions are satisfied by the cost function F in (4), as shown in the following lemma.

Lemma 1 (Submodularity of the cost function). *The set function maximized in Algorithm 1,*

$$F(\mathcal{S}) = \text{FP}(\Psi) - \text{FP}(\Psi_{\mathcal{N} \setminus \mathcal{S}}), \quad (6)$$

is a normalized, monotone, submodular function.

Proof: The set function F is normalized if $F(\emptyset) = 0$. Here, normalization is trivially shown since $\Psi = \Psi_{\mathcal{N}}$ by definition. To show monotonicity, we pick a generic matrix Ψ of N rows, a set \mathcal{X} and an index $i \notin \mathcal{X}$. Then, we compute the increment of F due to the element i w.r.t. to the set \mathcal{X} and we show that it is always positive.

$$\begin{aligned} F(\mathcal{X} \cup i) - F(\mathcal{X}) &= \text{FP}(\Psi_{\mathcal{N} \setminus \mathcal{X}}) - \text{FP}(\Psi_{\mathcal{N} \setminus \mathcal{X} \cup i}) \\ &\stackrel{(a)}{=} \sum_{n,m \in \mathcal{A} \cup i} |\langle \psi_n, \psi_m \rangle|^2 - \sum_{n,m \in \mathcal{A}} |\langle \psi_n, \psi_m \rangle|^2 \\ &= 2 \sum_{n \in \mathcal{A}} |\langle \psi_n, \psi_i \rangle|^2 + |\langle \psi_i, \psi_i \rangle|^2 \geq 0 \end{aligned}$$

where (a) is due to a change of variable $\mathcal{N} \setminus \mathcal{X} = \mathcal{A}$. We check the submodularity according to Definition 1 and assuming w.l.o.g. that $\mathcal{Y} = \mathcal{X} \cup j$.

$$\begin{aligned} & F(\mathcal{X} \cup i) - F(\mathcal{X}) - F(\mathcal{Y} \cup i) + F(\mathcal{Y}) \\ &= F(\mathcal{X} \cup i) - F(\mathcal{X}) - F(\mathcal{X} \cup \{i, j\}) + F(\mathcal{X} \cup j) \\ &= \text{FP}(\Psi_{\mathcal{A} \cup \{i, j\}}) - \text{FP}(\Psi_{\mathcal{A} \cup j}) - \text{FP}(\Psi_{\mathcal{A} \cup i}) + \text{FP}(\Psi_{\mathcal{A}}) \\ &= 2 \sum_{n \in \mathcal{A} \cup j} |\langle \psi_n, \psi_i \rangle|^2 - 2 \sum_{n \in \mathcal{A}} |\langle \psi_n, \psi_i \rangle|^2 \\ &= 2 |\langle \psi_i, \psi_j \rangle|^2 \geq 0. \end{aligned}$$

■

Now, we use Theorem 1 to derive the approximation factor of SmartSense w.r.t. the FP.

Theorem 2 (FP approximation factor). *Consider a matrix $\Psi \in \mathbb{R}^{N \times K}$ and a given number of sensors L , such that $K \leq L < N$. Denote the optimal set of locations as $\text{OPT} = \arg \max_{\mathcal{A} \subset \mathcal{N}, |\mathcal{A}|=L} \text{FP}(\Psi_{\mathcal{A}})$ and the greedy solution found by SmartSense as \mathcal{L} . Then, \mathcal{L} is near-optimal in a FP sense and*

$$\text{FP}(\Psi_{\mathcal{L}}) \leq \alpha \text{FP}(\Psi_{\text{OPT}}), \quad (7)$$

where $\alpha = \left(1 + \frac{1}{e} \left(\text{FP}(\Psi) \frac{K}{L_{\text{MIN}}^2} - 1\right)\right)$ is the approximation factor and $L_{\text{MIN}} = \min_{|\mathcal{L}|=L} \sum_{i \in \mathcal{L}} \|\psi_i\|^2$ is the sum of the norms of the L rows with the smallest norm.

Proof: According to Lemma 1, the cost function used in SmartSense satisfies the conditions of Theorem 1. Therefore,

$$F(\overline{\text{OPT}}) - F(\mathcal{S}) \leq \frac{1}{e} (F(\overline{\text{OPT}})),$$

where $F(\mathcal{S}) = \text{FP}(\Psi) - \text{FP}(\Psi_{\mathcal{N} \setminus \mathcal{S}})$ is the considered cost function, \mathcal{S} is the set of rows eliminated by SmartSense and $\overline{\text{OPT}} = \mathcal{N} \setminus \text{OPT}$. Plugging in the cost function, we obtain

$$\text{FP}(\Psi_{\mathcal{N} \setminus \mathcal{S}}) \leq \left(1 - \frac{1}{e}\right) \text{FP}(\Psi_{\mathcal{N} \setminus \overline{\text{OPT}}}) + \frac{1}{e} \text{FP}(\Psi). \quad (8)$$

Then, we note that the following minimization problem,

$$\begin{aligned} & \text{minimize}_{\mathcal{L}} && \text{FP}(\Psi_{\mathcal{L}}) \\ & \text{subject to} && |\mathcal{L}| = L \end{aligned}$$

is equivalent, under the change of variable $\mathcal{L} = \mathcal{N} \setminus \mathcal{S}$, to

$$\begin{aligned} & \text{minimize}_{\mathcal{S}} && \text{FP}(\Psi_{\mathcal{N} \setminus \mathcal{S}}) \\ & \text{subject to} && |\mathcal{S}| = N - L \end{aligned}$$

Using this in (8), we obtain

$$\text{FP}(\Psi_{\mathcal{L}}) \leq \left(1 + \frac{1}{e} \left(\frac{\text{FP}(\Psi)}{\text{FP}(\Psi_{\text{OPT}})} - 1\right)\right) \text{FP}(\Psi_{\text{OPT}})$$

To conclude the proof, we bound from above the term $\frac{1}{e} \frac{\text{FP}(\Psi)}{\text{FP}(\Psi_{\text{OPT}})}$. First, we consider the optimal solution OPT to select a tight frame whose rows have a summed norm of $L_{\text{OPT}} = \sum_{i \in \text{OPT}} \|\psi_i\|^2$,

$$\text{FP}(\Psi_{\mathcal{L}}) \leq \left(1 + \frac{1}{e} \left(\text{FP}(\Psi) \frac{K}{L_{\text{OPT}}^2} - 1\right)\right) \text{FP}(\Psi_{\text{OPT}}).$$

We conclude the proof assuming that the optimal selection

is also the one selecting the rows having the smallest norm, $L_{\text{OPT}} \geq L_{\text{MIN}} = \min_{|\mathcal{L}|=L} \sum_{i \in \mathcal{L}} \|\psi_i\|^2$. ■

Note that the FP of the original matrix influences significantly the final result: the lower the FP of Ψ , the tighter the approximation obtained by the greedy algorithm. Therefore, SmartSense performs better when the original matrix Ψ is closer to a tight frame. Moreover, Theorem 2 suggests to remove from Ψ the rows whose norm is significantly smaller w.r.t. the others to improve the performance of SmartSense. This suggestion has an intuitive explanation, since such rows are also the less *informative*.

C. Near-optimality of SmartSense w.r.t. MSE

Having a near-optimal FP does not necessarily mean that the obtained MSE is also close to the optimal one. In this section, we show that under some assumptions on the spectrum of Ψ , SmartSense is near optimal w.r.t. MSE as well.

Before going further into technical details, we generalize the concept of number of sensors to account for the norms of the rows of Ψ . More precisely, we keep L as the number of rows while we define $L_{\text{SUM}} = \sum_{i \in \mathcal{A}} \|\psi_i\|^2$ as the sum of the norms of the rows of $\Psi_{\mathcal{A}}$ for a generic set \mathcal{A} . We also define the two extremal values of L_{SUM} ,

$$L_{\text{MIN}} = \min_{\mathcal{A} \in \mathcal{N}, |\mathcal{A}|=L} \sum_{i \in \mathcal{A}} \|\psi_i\|^2 \quad (9)$$

$$L_{\text{MAX}} = \max_{\mathcal{A} \in \mathcal{N}, |\mathcal{A}|=L} \sum_{i \in \mathcal{A}} \|\psi_i\|^2, \quad (10)$$

indicating respectively the minimum and the maximum value of L_{SUM} among all possible selections of L out of N rows of Ψ . L_{SUM} is also connected to the spectrum of $\mathbf{T}_{\mathcal{A}}$. Indeed, L_{SUM} is the trace of $\mathbf{T}_{\mathcal{A}}$ and thus it is also the sum of its eigenvalues,

$$L_{\text{SUM}} = \sum_{i \in \mathcal{A}} \|\psi_i\|^2 = \text{Trace}(\mathbf{T}_{\mathcal{A}}) = \sum_{i \in \mathcal{A}} \lambda_i.$$

Finally, note that if Ψ has rows with unit-norm, then $L_{\text{SUM}} = L_{\text{MIN}} = L_{\text{MAX}} = L$.

As a first step to prove the near-optimality w.r.t. MSE, we consider a possible placement \mathcal{A} and we bound the MSE of the matrix $\Psi_{\mathcal{A}}$ using its FP and the spectrum of $\mathbf{T}_{\mathcal{A}}$. To obtain such bound, we use a known inequality [23] involving variance, arithmetic mean and harmonic mean of a set of positive bounded numbers, in this case the eigenvalues of $\mathbf{T}_{\mathcal{A}}$. The following lemma describes the bound, while its proof is given in Appendix A.

Lemma 2 (MSE bound). *Consider any $\Psi_{\mathcal{A}} \in \mathbb{R}^{L \times K}$ with $L \leq K$, obtained from Ψ for $|\mathcal{A}| = L$, with a frame potential $\text{FP}(\Psi_{\mathcal{A}})$. Denote the spectrum of $\mathbf{T}_{\mathcal{A}}$ as $\lambda_1 \geq \dots \geq \lambda_K$. Then the MSE is bounded as follows*

$$\text{MSE}(\Psi_{\mathcal{A}}) \leq \frac{K}{L_{\text{MIN}}} \frac{\text{FP}(\Psi_{\mathcal{A}})}{\lambda_K^2}, \quad (11)$$

$$\text{MSE}(\Psi_{\mathcal{A}}) \geq \frac{K}{L_{\text{MAX}}} \frac{\text{FP}(\Psi_{\mathcal{A}})}{\lambda_1^2}, \quad (12)$$

where L_{MIN} and L_{MAX} are defined in (9) and (10).

Lemma 2 is key to study the approximation factor w.r.t. MSE. Specifically, it allows to analyze the two extremal cases:

- given the optimal FP, what is the lowest MSE we can achieve?
- given the worst case FP according to Theorem 2, what is the largest MSE we may encounter?

Lemma 2 implies the necessity to properly bound the spectrum of any $\Psi_{\mathcal{A}}$ with a given FP obtained from Ψ . While it is possible to bound λ_1 with the FP, it is also easy to build matrices with $\lambda_K = 0$ compromising the bound given in (11). Therefore, we introduce the following property to control the eigenvalues of any $\mathbf{T}_{\mathcal{A}}$.

Definition 2 ((δ, L) -bounded frame). *Consider a matrix $\Psi \in \mathbb{R}^{N \times K}$ where $N \geq L$ and $N > K$. Then, we say that Ψ is (δ, L) -bounded if for every $\mathcal{A} \subseteq \mathcal{N}$ such that $|\mathcal{A}| = L$, $\mathbf{T}_{\mathcal{A}}$ has a bounded spectrum*

$$\frac{L_{MEAN}}{K} - \delta \leq \lambda_i \leq \frac{L_{MEAN}}{K} + \delta,$$

where $1 \leq i \leq K$, $\delta \geq 0$ and $L_{MEAN} = \frac{L}{N} \sum_{i \in \mathcal{N}} \|\psi_i\|^2$ is average value of L_{SUM} .

The concept of (δ, L) -bounded frames is similar to the notion of RIP matrices used in compressive sensing to guarantee the reconstruction of a sparse vector from a limited number of linear measurements [24]. Moreover, it allows us to define an approximation factor for the MSE that does not depend on the FP, the cost-function we minimize.

Theorem 3 (MSE approximation factor for (δ, L) -bounded frames). *Consider a matrix $\Psi \in \mathbb{R}^{N \times K}$ and $L \geq K$ sensors. Assume Ψ to be a (δ, L) -bounded frame, let d be the ratio L_{MEAN}/K and define the optimal allocation in terms of MSE as $OPT = \arg \min_{\mathcal{A} \in \mathcal{N}, |\mathcal{A}|=L} \text{MSE}(\Psi_{\mathcal{A}})$. Then the solution \mathcal{L} of SmartSense is near-optimal w.r.t. MSE,*

$$\text{MSE}(\Psi_{\mathcal{L}}) \leq \beta \text{MSE}(\Psi_{OPT}) \text{ with } \beta = \alpha \frac{(d + \delta)^2 L_{MAX}}{(d - \delta)^2 L_{MIN}},$$

where β is the approximation factor of the MSE and α is the approximation factor of the FP.

Proof: First, we compute the worst case MSE when SmartSense yields the worst FP, that is for $\text{FP}(\Psi_{\mathcal{L}}) = \alpha \text{FP}(\Psi_{OPT})$, using the upper bound (11) and the bounds on the spectrum for (δ, L) -bounded frames,

$$\text{MSE}(\Psi_{\mathcal{L}}) \leq \frac{K}{L_{MIN}} \frac{\alpha \text{FP}(\Psi_{OPT})}{(d - \delta)^2}. \quad (13)$$

Then, we compute the best case MSE when the FP is optimal. We note that the lower bound (12) of the MSE is monotonically decreasing w.r.t. the FP. Therefore, we use the previous simple strategy on the lower bound,

$$\text{MSE}(\Psi_{OPT}) \leq \frac{K}{L_{MAX}} \frac{\text{FP}(\Psi_{OPT})}{(d + \delta)^2}. \quad (14)$$

Note that we consider the optimal MSE to be achieved for the optimal FP because the lower bound of the MSE is monotonically decreasing w.r.t. to FP. Finally, we compute the MSE approximation ratio, as the ratio between (13) and

(14), obtaining the desired result. \blacksquare

Here, the key is the definition of (δ, L) -bounded frames. It turns out that many families of random matrices adequately normalized satisfy Definition 2, but it is very hard to build deterministic matrices with such spectral properties. Nonetheless, as is the case for compressed sensing and RIP matrices [25], SmartSense works well even for Ψ that are not (δ, L) -bounded.

IV. NUMERICAL RESULTS

In this section, we analyze the performance of SmartSense and compare it with the state-of-the-art algorithms for sensor placement.

A. Synthetic data

First, we compare the FP with other cost functions when used in a naive greedy algorithm. Among the one listed in Section I-B, we select the following four cost functions: entropy [12], mutual information [14], determinant of $\mathbf{T}_{\mathcal{L}}$ [5], and MSE [15]. We also consider an algorithm that randomly allocates the sensors to relate the obtained results to a random selection.

The greedy algorithms are tested on different types of sensing matrices Ψ :

- random matrices with Gaussian i.i.d. entries,
- random matrices with Gaussian i.i.d. entries whose rows are normalized,
- random matrices with Gaussian i.i.d. entries with orthonormalized columns,
- DCT matrices of size N where $N - K$ columns are randomly discarded.

We considered $\Psi \in \mathbb{R}^{100 \times 20}$ and evaluated the performance in terms of MSE for $L = \{30, 35, 40, 45, 50, 55, 60\}$. We considered 20 different instances⁴ for each combination, and we plotted the average MSE as a function of L . The results are given in Figure 2. We note that SmartSense is consistently outperforming all other cost functions. For the random Gaussian matrices case, mutual information shows similar results. However, looking at subsampled DCT matrices, we see that mutual information leads to a significantly worse MSE. Note that certain cost functions show worse performance than a random selection of the rows. While this phenomena could be partially explained by the special properties of certain families of random matrices, it indicates the importance of choosing a well-studied cost function for which we can obtain performance bounds w.r.t. to the MSE.

In the second experiment, we compare SmartSense with the state-of-the-art method based on convex optimization [6]. Since the algorithm proposed by Joshi et al. is structurally different from SmartSense, we focus this analysis on two parameters: the computational time and the MSE. We fix $K = 20$ and the ratio between the number of sensors and the number of available locations as $L/N = 0.5$. Then, we vary the

⁴The relatively small size of Ψ and the small number of trials are due to the lack of scalability of certain cost functions, that require the computation of large matrices.

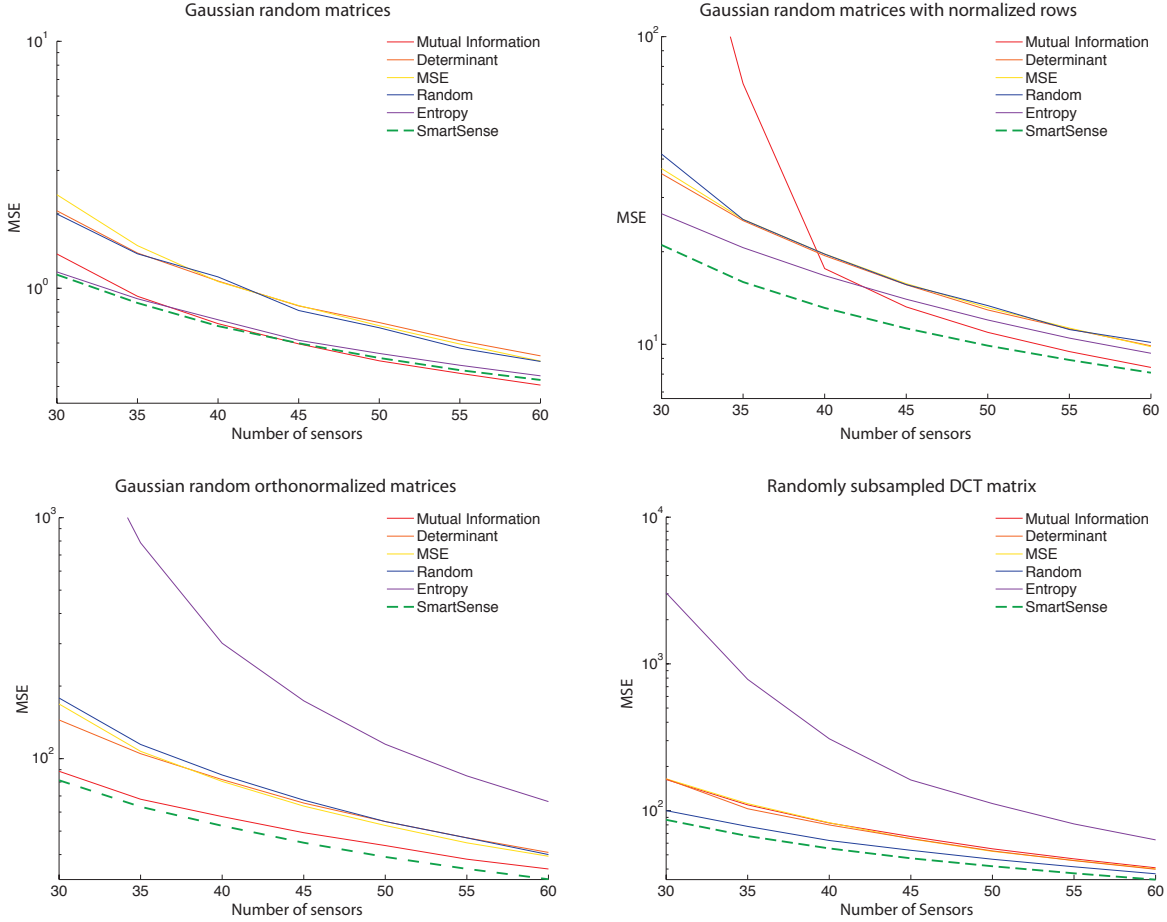


Fig. 2. Performance comparison between SmartSense and other greedy algorithms using commonly considered cost functions. We randomly generated matrices with $N = 100$ and $K = 20$ and tested varying number of sensors with different greedy algorithms. The performance is measured in terms of MSE, so the lower the curve, the higher the performance. We considered four different types of sensing matrices, and in all cases SmartSense outperformed the other algorithms. We underline the consistency of SmartSense over the four types of matrices. Indeed, even if the mutual information is slightly better than SmartSense for Gaussian random matrices, it shows poor results for the other matrices.

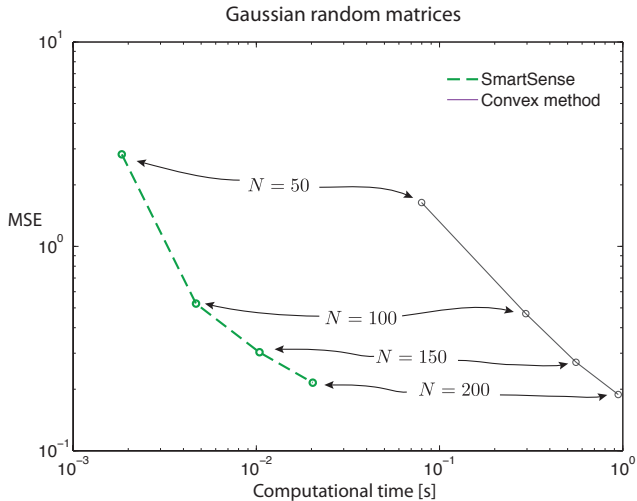


Fig. 3. Analysis of the tradeoff between computational time and MSE for SmartSense and the convex relaxed algorithm proposed by Joshi et al. [6]. We generated 30 Gaussian matrices with $K = 20$ and of increasing size $N = \{50, 100, 150, 200\}$, while we placed $L = 0.5N$ sensors. We measured the average computational time together with the average MSE, showing that while SmartSense is significantly faster than the convex algorithm, the difference in MSE is minimal. Moreover, the gap in the quality of the solution decreases for an increasing size of the problem N .

number of possible locations as $N = \{50, 100, 150, 200\}$. The results for Gaussian random matrices are given in Figure 3. First, we note that the convex method achieves a lower MSE, however the performance gap decreases when we increase the number of sensors. This is not surprising, since SmartSense is a greedy algorithm that does not require parameter fine-tuning nor heuristics, while the convex relaxation method integrates some efficient heuristics. For example, at every iteration it refines the selection by looking at all the possible *swaps* between the chosen location and the discarded ones. This strategy is particularly effective when $L \approx K$: in fact, swapping just one row can improve significantly the spectrum of $\mathbf{T}_{\mathcal{L}}$, and consequently the MSE achieved by $\Psi_{\mathcal{L}}$. The heuristics, while being effective in terms of MSE, increase also the computational cost. In fact, SmartSense is almost 100 times faster.

The last comparison also opens an interesting direction for future work. In fact, the convex relaxed algorithm optimizes the determinant of $\mathbf{T}_{\mathcal{L}}$ and its near-optimality in terms of MSE has not been shown. Moreover, this cost function has been proven to be less effective compared to FP when used in a greedy algorithm (see Figure 2). Therefore, we expect that a convex relaxed scheme based on the FP has the potential to

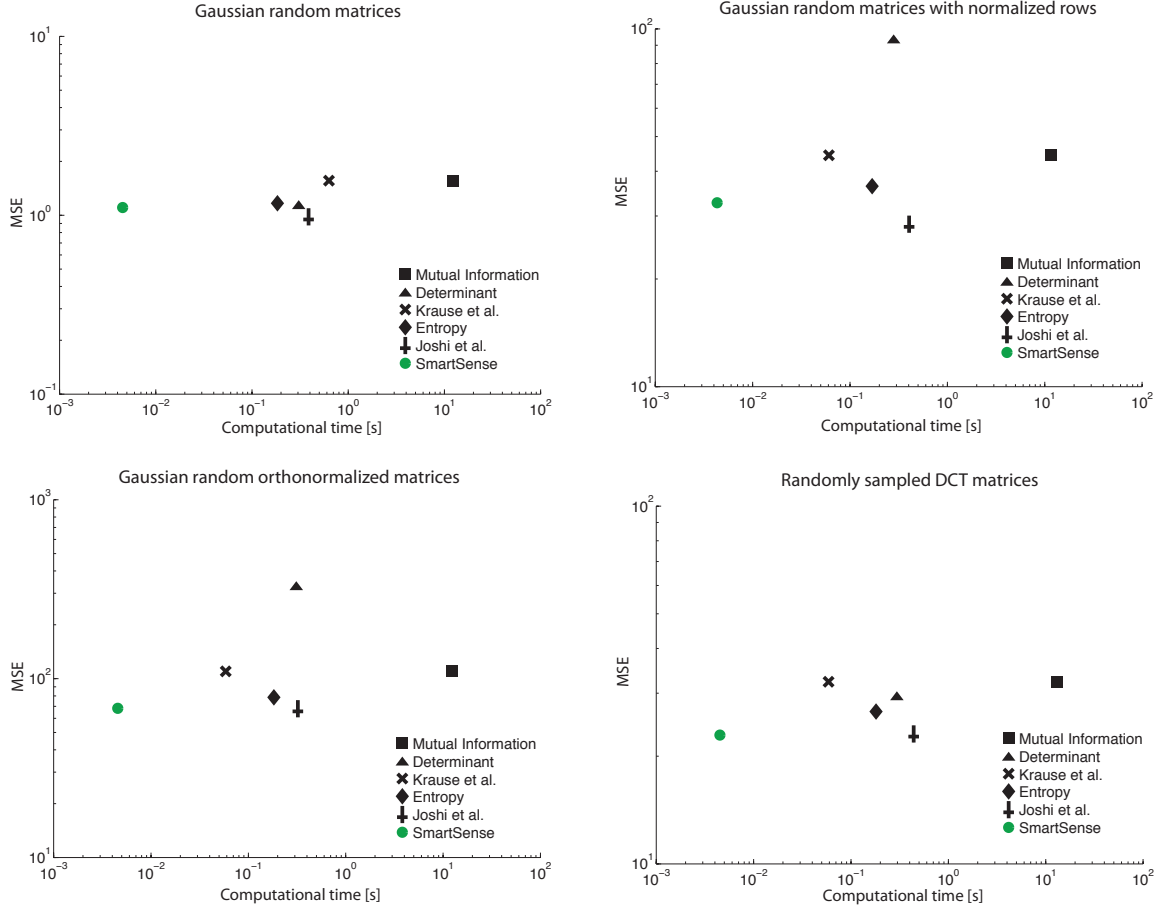


Fig. 4. Tradeoff between computational time and MSE. We randomly generated matrices—according to four different models—with $N = 100$, $K = 30$ and $L = 50$ sensors. The performance is measured in terms of MSE, therefore the lower the dot, the higher the performance. On the other hand, the computational time is measured in seconds. Note that, SmartSense is the fastest algorithm by one order of magnitude and it is the second best algorithm in terms of MSE. When the legend refer to a cost function, we considered a naive greedy algorithm optimizing that cost function. On the other hand, we refer to the authors for specific algorithms implementing complicated schemes and/or heuristics.

define a new state-of-the-art, mixing the advantages of FP and the heuristics proposed in [6].

To conclude the performance analysis, we study the trade-off between computational complexity and performance for all the considered algorithms, greedy and not. We also consider the lazy greedy algorithm optimizing the mutual information proposed by Krause et al. [14], since it reduces the number of evaluated locations by avoiding the ones close to the already selected locations⁵. We picked 20 instances of each of the random matrices proposed in the first experiment with $N = 100$, $L = 50$ and $K = 30$. We measured the average computational time and average MSE obtained by each algorithm and the results are given in Figure 4. We note a general trend connecting the four subfigures: SmartSense is the fastest algorithm, by at least an order of magnitude, while its performance is just second, as previously shown, to the convex relaxed method proposed by Joshi et al. [6].

An opportune critic to the computational cost analysis is the following: sensor allocation is an off-line procedure and computational time is of secondary importance. While this is true in many applications, there are certain applications where

⁵Due to issues of the lazy algorithm with rank deficient matrices, we just measured its computational time and optimistically considered the MSE of the naive greedy algorithm.

it is necessary to recompute \mathcal{L} regularly. This is usually the case when Ψ changes in time due to changes of the physical field and it is possible to adaptively reallocate the sensors. In other applications, such as the ones where we attempt to interpolate the entire field from L measurements, the number of possible locations N grows with the desired resolution. In this case, a lower computational time is of critical importance.

B. Temperature estimation on many-core processors

We now analyze the impact of SmartSense on a well-known real-world problem where sensor allocation is of fundamental importance. We describe the problem briefly, followed up by a simulation showing the improvement w.r.t. the state-of-the-art.

The continuous evolution of process technology increases the performance of processors by including more cores memories and complex interconnection fabrics on a single chip. Unfortunately, a higher density of components increases the power densities and amplifies the concerns for thermal issues. In particular, it is key to design many-core processors that prevent hot spots and large on-chip temperature gradients, as both conditions severely affect the overall system’s characteristics. A non-exhaustive list of problems induced by thermal stress includes higher failure rate, reduced performance, increased

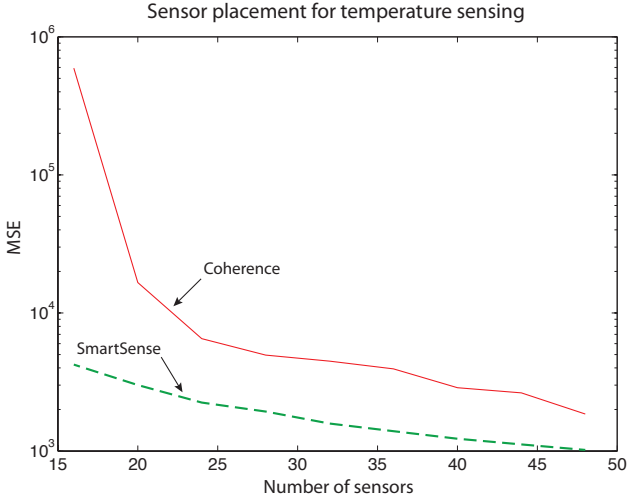


Fig. 5. Comparison between SmartSense and a coherence-based greedy algorithm proposed in [30]. In this experiment, we consider the sensors placement to estimate the temperature of an 8-core microprocessor using a limited number of sensors. The matrix $\Psi \in \mathbb{R}^{3360 \times 16}$ is generated from a principal component analysis of known thermal maps and it is the same considered in [30]. Note that SmartSense significantly outperforms the previous method, in particular when the number of sensors is close to the number of estimated parameters. This is of fundamental importance: while we cannot further reduce the number of parameters since it would significantly degrade the reconstruction performance, we can reduce the number of sensors, implying a reduction of their area and power consumption.

power consumption due to current leakage and increased cooling costs. To overcome these issues, the latest designs include the thermal information into the workload allocation strategy to obtain optimal performance while avoiding critical thermal scenarios. Consequently, a few sensors are deployed on the chip to collect data about the thermal status. However, their number is limited by area/power constraints and their optimal placement to detect all the worst-case temperature scenarios is still unresolved and has received significant attention [8, 26–29].

An improvement of the sensor allocation techniques would lead to a reduction of the sensing cost in terms of used silicon surface. Moreover, it implies a reduction of the reconstruction error, making possible the use of more aggressive scheduling strategies and consequently improves the processor performance. In [30], we proposed the following strategy: learn Ψ using a principal component analysis on an extensive set of thermal maps, then place the sensors with a greedy algorithm minimizing the coherence between the rows. This work achieved a significant improvement w.r.t. the previous state-of-the-art approach [27].

We consider the same matrix Ψ used in [30] and we compared our previous greedy algorithm with SmartSense. The results are shown in Figure 5. We note that the performance of the placement algorithm has been further improved by SmartSense, without increasing the computational cost nor changing the reconstruction strategy. Moreover, we are now able to guarantee the near-optimality of the algorithm w.r.t. the MSE of the estimated thermal map.

V. CONCLUSIONS

In this paper we studied the optimization of the sensor placement when the collected measurements are used to solve

a linear inverse problem. The problem is equivalent to choose L rows out of N from a matrix Ψ such that the obtained matrix has favorable spectral properties. The problem is intrinsically combinatorial and approximation algorithms are necessary for plausible real-world scenarios. While many approximation algorithms are available in the prior art, none of them has guaranteed performance in terms of the MSE of the solution of the inverse problem, the key merit figure for such problem.

We proposed SmartSense, a greedy worst-out algorithm minimizing the frame potential. Even if the chosen cost function is well-known in frame theory for its fundamental role in the construction of frames with optimal MSE, SmartSense is the first algorithm exploiting it. Our theoretical analysis demonstrate the following innovative aspects:

- SmartSense is near-optimal w.r.t. the frame potential, meaning that it always places the sensors such that the obtained frame potential is guaranteed to be close to the optimal one.
- under RIP-like assumptions for Ψ , SmartSense is also near-optimal w.r.t. the MSE. Note that SmartSense is the first algorithm in literature having such important aspect.

We provided extensive numerical experiments showing that SmartSense achieves the best performance in terms of MSE while having the lowest computational complexity when compared to many other greedy algorithms. SmartSense is also competitive performance-wise with the state-of-the-art algorithm based on a convex relaxation proposed in [6], while keeping a significant advantage in terms of computational time.

We showed that SmartSense represents the new state-of-the-art on a real-world scenario, the reconstruction of thermal maps of many-core processors. This improvement leads to a potential reduction of the number of sensors required to estimate precisely the thermal distribution, reducing the area occupied and the power consumed by the sensors.

Future work will be two-fold. First, it is imaginable to relax the RIP-like condition on Ψ by considering that the characteristics of the frame potential are potentially sufficient to avoid the $\Psi_{\mathcal{L}}$ with the unfavorable spectral distribution. Second, we believe that a convex relaxed scheme based on the frame potential integrating the heuristics proposed by Joshi et al. [6] could improve significantly the MSE of the obtained solution, while keeping the near-optimality due to the frame potential.

APPENDIX

A. Bounding the MSE with the frame potential

In this section, we bound the MSE of a matrix $\Psi_{\mathcal{A}} \in \mathbb{R}^{L \times K}$ as a function of its FP and the spectrum $\{\lambda_i\}_{i=1}^K$ of $\mathbf{T}_{\mathcal{L}}$.

First, consider the harmonic mean $H = \frac{K}{\sum_k \frac{1}{\lambda_j}}$, the arithmetic mean $A = \frac{\sum_k \lambda_k}{K}$ and the standard deviation $S = \sqrt{\frac{1}{K} \sum_k (\lambda_k - A)^2}$ of the eigenvalues of $\mathbf{T}_{\mathcal{L}}$. All these quantities are linked to $\text{MSE}(\Psi_{\mathcal{A}})$, the number of sensors L

and $\text{FP}(\Psi_{\mathcal{A}})$. More precisely, we have

$$\begin{aligned} H &= \frac{K}{\text{MSE}(\Psi_{\mathcal{A}})}, \\ A &= \frac{L_{\text{SUM}}}{K}, \\ S &= \sqrt{\frac{1}{K} \left(\text{FP}(\Psi_{\mathcal{A}}) - \frac{L_{\text{SUM}}^2}{K} \right)}. \end{aligned}$$

Then, we consider the following bounds for the harmonic mean of a set of positive numbers derived by Sharma [23],

$$\frac{(M-S)^2}{M(M-2S)} \leq \frac{A}{H} \leq \frac{(m+S)^2}{m(m+2S)},$$

where m and M are the smallest and the largest number in the set. We use the expressions of A and H and we remove the mixed term in the denominator to obtain,

$$\frac{K^2}{L_{\text{SUM}}} \left(1 + \frac{S^2}{M^2} \right) \leq \text{MSE}(\Psi_{\mathcal{A}}) \leq \frac{K^2}{L_{\text{SUM}}} \left(1 + \frac{S^2}{m^2} \right).$$

As expected when the FP achieves its global minima, that is $S = 0$, we achieve the optimal MSE of a tight frame.

To conclude the proof, we consider the two bounds separately starting from the lower one. Let $M = \lambda_1$ and we plug in the value of S . We also consider w.l.o.g. $L_{\text{SUM}} \leq L_{\text{MAX}}$, since we can always improve the MSE by increasing the sensing power L_{SUM} . Then,

$$\text{MSE}(\Psi_{\mathcal{L}}) \geq \frac{K^2}{L_{\text{MAX}}} \left(1 + \frac{\text{FP}(\Psi_{\mathcal{A}})}{K\lambda_1^2} - \frac{L_{\text{MAX}}^2}{K^2\lambda_1^2} \right).$$

We obtain the final result by using lower bound on the largest eigenvalue: $\lambda_1 \geq \frac{L_{\text{MAX}}}{K}$.

The approach to prove the upper bound is exactly symmetrical. Specifically, consider $m = \lambda_N$, $L_{\text{SUM}} \geq L_{\text{MIN}}$ and use the upper bound on the smallest eigenvalue $\lambda_N \leq \frac{L_{\text{MAX}}}{K}$.

ACKNOWLEDGMENT

The authors would like to thank Ivan Dokmanić and Prof. Ola Svensson whose suggestions were fundamental to strengthen the results described in the paper. This research was supported by an ERC Advanced Grant – Support for Frontier Research – SPARSAM Nr: 247006.



Juri Ranieri received both his M.S. and B.S. degree in Electronic Engineering in 2009 and 2007, respectively, from Università di Bologna, Italy. From July to December 2009, he joined as a visiting student the Audiovisual Communications Laboratory (LCAV) at EPF Lausanne, Switzerland. From January 2010 to August 2010, he was with IBM Zurich to investigate the lithographic process as a signal processing problem. From September 2010, he is in the doctoral school at EPFL where he joined LCAV under the supervision of Prof. Martin Vetterli and Dr. Amina

Chebira. From April 2013 to July 2013, he was an intern at Lyric Labs of Analog Devices, Cambridge, USA. His main research interests are inverse problems of physical fields and the spectral factorization of autocorrelation functions.



Amina Chebira is a scientific researcher at the Swiss Center for Electronics and Microtechnology (CSEM) in Neuchâtel, Switzerland. She received the M.S. degree in communication systems from the Ecole Polytechnique Federale de Lausanne (EPFL) in 2003 and the Ph.D. degree from the Biomedical Engineering Department, Carnegie Mellon University, Pittsburgh, PA, in 2008, for which she received the BME research award. Successively, she held a Postdoctoral Researcher position at the with the Audiovisual Communications Laboratory, EPFL, where

she was also from 2003 to 2004 as a scientific assistant.

From March 2003 to September 2003, she was an intern at Philips Research Laboratories (Nat.Lab) in Eindhoven, The Netherlands. In September 1998, she obtained a Bachelor degree in mathematics from University Paris 7 Denis Diderot. Her research interests include frame theory and design, biomedical signal processing, and pattern recognition.



Martin Vetterli (S86M86SM90F95) received the Dipl. El.-Ing. degree from ETH Zurich (ETHZ), Switzerland, in 1981, the MS degree from Stanford University in 1982, and the Doctorat en Sciences degree from EPF Lausanne (EPFL), Switzerland, in 1986. He was a research assistant at Stanford and EPFL, and has worked for Siemens and AT&T Bell Laboratories. In 1986 he joined Columbia University in New York, where he was last an Associate Professor of Electrical Engineering and co-director of the Image and Advanced Television Laboratory. In 1993,

he joined the University of California at Berkeley, where he was a Professor in the Department of Electrical Engineering and Computer Sciences until 1997, and has held an Adjunct Professor position until June 2010. Since 1995 he is a Professor of Communication Systems at EPF Lausanne, Switzerland, where he chaired the Communications Systems Division (1996/97), and heads the Audiovisual Communications Laboratory. From 2001 to 2004 he directed the National Competence Center in Research on mobile information and communication systems. He also was a Vice-President at EPFL from October 2004 to February 2011 in charge, among others, of international affairs and computing services. He has held visiting positions at ETHZ (1990) and Stanford (1998). From March 2011 to December 2012, he was Dean of the School of Computer and Communication Sciences of EPFL. Since January 2013, he leads the Swiss National Science Foundation. He is a fellow of IEEE, a fellow of ACM, a fellow of EURASIP, and a member of SIAM. He is on the editorial boards of Applied and Computational Harmonic Analysis, the Journal of Fourier Analysis and Application and the IEEE Journal on Selected Topics in Signal Processing. He received the Best Paper Award of EURASIP in 1984, the Research Prize of the Brown Boverly Corporation (Switzerland) in 1986, the IEEE Signal Processing Society Senior Paper Awards in 1991, in 1996 and in 2006 (for papers with D. LeGall, K. Ramchandran, and Marziliano and Blu, respectively). He won the Swiss National Latsis Prize in 1996, the SPIE Presidential award in 1999, the IEEE Signal Processing Technical Achievement Award in 2001, the IEEE Signal Processing Society Award in 2010 and is an ISI highly cited researcher in engineering. He was a member of the Swiss Council on Science and Technology from 2000 to 2003. He was a plenary speaker at various conferences (e.g. IEEE ICIP, ICASSP, ISIT) and is the co-author of three books with J. Kovacevic, Wavelets and Subband Coding, 1995, with P. Prandoni Signal Processing for Communications, 2008 and with J. Kovacevic and V.K. Goyal, Foundations of Signal Processing, 2012. He has published about 150 journal papers on a variety of topics in signal/image processing and communications and holds two dozen patents. His research interests include sampling, wavelets, multirate signal processing, computational complexity, signal processing for communications, digital image/video processing, joint source/channel coding, signal processing for sensor networks and inverse problems like acoustic tomography.

REFERENCES

- [1] M. Vetterli, P. Marziliano, and T. Blu, "Sampling signals with finite rate of innovation," *IEEE Trans. Signal Process.*, vol. 50, no. 6, pp. 1417–1428, 2002.
- [2] R. G. Baraniuk and M. B. Wakin, "Random projections of smooth manifolds," *Found. Comput. Math.*, vol. 9, no. 1, pp. 51–77, 2009.
- [3] A. M. Bruckstein, D. L. Donoho, and M. Elad, "From sparse solutions of systems of equations to sparse modeling of signals and images," *SIAM Review*, vol. 51, no. 1, pp. 34–81, 2009.
- [4] M. Fickus, D. G. Mixon, and M. J. Poteet, "Frame completions for optimally robust reconstruction," *arXiv*, July 2011.
- [5] M. Shamaiah, S. Banerjee, and H. Vikalo, "Greedy sensor selection: leveraging submodularity," in *CDC*, 2010.
- [6] S. Joshi and S. Boyd, "Sensor selection via convex optimization," *IEEE Trans. Signal Process.*, vol. 57, no. 2, pp. 451–462, 2009.
- [7] M. Al-Obaidy, A. Ayesh, and A. F. Sheta, "Optimizing the communication distance of an ad hoc wireless sensor networks by genetic algorithms," *Artif. Intell. Rev.*, vol. 29, no. 3-4, June 2008.
- [8] R. Mukherjee and S. Memik, "Systematic temperature sensor allocation and placement for microprocessors," in *DAC*, Anaheim, USA, 2006.
- [9] S. Lau, R. Eichardt, L. Di Rienzo, and J. Haueisen, "Tabu search optimization of magnetic sensor systems for magnetocardiography," *IEEE Trans. Magn.*, vol. 44, no. 6, pp. 1442–1445, 2008.
- [10] P. L. Chiu and F. Y. S. Lin, "A simulated annealing algorithm to support the sensor placement for target location," in *Can. Con. El. Comp. En.* 2004, pp. 867–870, IEEE.
- [11] D. J. C. MacKay, "Information-based objective functions for active data selection," *Neural Comput.*, vol. 4, no. 4, pp. 590–604, 1992.
- [12] H. Wang, G. Pottie, K. Yao, and D. Estrin, "Entropy-based sensor selection heuristic for target localization," in *IPSN*. 2004, pp. 36–45, ACM.
- [13] G. Nemhauser, L. Wolsey, and M. Fisher, "An analysis of approximations for maximizing submodular set functions—I," *Math. Prog.*, vol. 14, no. 1, pp. 265–294, 1978.
- [14] A. Krause, A. Singh, and C. Guestrin, "Near-optimal sensor placements in Gaussian processes: Theory, efficient algorithms and empirical studies," *JMLR*, vol. 9, pp. 235–284, 2008.
- [15] A. Das and D. Kempe, "Algorithms for Subset Selection in Linear Regression," in *STOC*. 2008, pp. 45–54, ACM.
- [16] M. Naem, S. Xue, and D. C. Lee, "Cross-Entropy optimization for sensor selection problems," in *ISCIT*. 2009, pp. 396–401, IEEE.
- [17] D. Golovin, M. Faulkner, and A. Krause, "Online distributed sensor selection," *arXiv*, Feb. 2010.
- [18] N. Ramakrishnan, C. Bailey-Kellogg, S. Tadepalli, and V. N. Pandey, "Gaussian processes for active data mining of spatial aggregates," in *SDM*. 2005, p. 427, Society for Industrial Mathematics.
- [19] D. M. Steinberg and W. G. Hunter, "Experimental design: review and comment," *Technometrics*, vol. 26, no. 2, pp. 71–97, 1984.
- [20] V. K. Goyal, M. Vetterli, and N. Thao, "Quantized overcomplete expansions in \mathbb{R}^N : Analysis, synthesis, and algorithms," *IEEE Trans. Inf. Theory*, vol. 44, no. 1, pp. 16–31, 1998.
- [21] J. Benedetto and M. Fickus, "Finite normalized tight frames," *Adv. Comput. Math.*, vol. 18, no. 2, pp. 357–385, 2003.
- [22] P. G. Casazza, M. Fickus, J. Kovačević, M. Leon, and J. Tremain, "A physical interpretation of tight frames," in *Harmonic analysis and applications*, pp. 51–76. Springer, 2006.
- [23] R. Sharma, "Some more inequalities for arithmetic mean, harmonic mean and variance," *J. Math. Inequal.*, vol. 2, pp. 109–114, 2008.
- [24] E. J. Candes and M. B. Wakin, "An introduction to compressive sampling," *IEEE Signal Process. Mag.*, vol. 25, no. 2, pp. 21–30, 2008.
- [25] H. Monajemi, S. Jafarpour, M. Gavish, D. L. Donoho, S. Ambikasaran, S. Bacallado, D. Bharadia, Y. Chen, Y. Choi, and M. Chowdhury, "Deterministic matrices matching the compressed sensing phase transitions of Gaussian random matrices," *PNAS*, vol. 110, no. 4, pp. 1181–1186, 2013.
- [26] R. Cochran and S. Reda, "Spectral techniques for high-resolution thermal characterization with limited sensor data," in *DAC*, San Francisco, USA, June 2009, pp. 478–483, IEEE.
- [27] A. N. Nowroz, R. Cochran, and S. Reda, "Thermal monitoring of real processors: techniques for sensor allocation and full characterization," in *DAC*, New York, USA, 2010, p. 56, ACM Press.
- [28] S. Reda, R. Cochran, and A. N. Nowroz, "Improved thermal tracking for processors using hard and soft sensor allocation techniques," *IEEE Trans. Comput.*, vol. 60, no. 6, pp. 841–851, Nov. 2011.
- [29] S. Sharifi and T. Š. Rosing, "Accurate direct and indirect on-chip temperature sensing for efficient dynamic thermal management," *IEEE Trans. Comput.-Aided Des. Integr. Circuits Syst.*, vol. 29, no. 10, pp. 1586–1599, Oct. 2010.
- [30] J. Ranieri, A. Vincenzi, A. Chebira, D. Atienza, and M. Vetterli, "EigenMaps: algorithms for optimal thermal maps extraction and sensor placement on multicore processors," in *DAC*, San Francisco, June 2012, ACM Request Permissions.